Inorg. Chem. **2003**, *42*, 4098–4101

Kinetics and Mechanism of Iron(III)–Nitrilotriacetate Complex Reactions with Phosphate and Acetohydroxamic Acid

Mario Gabričević and Alvin L. Crumbliss*

Department of Chemistry, Duke University, Box 90346, Durham, North Carolina 27708-0346

Received December 17, 2002

The kinetics and mechanism of the substitution of coordinated water in nitrilotriacetate complexes of iron(III) ($Fe(NTA)(OH_2)_2$ and $Fe(NTA)(OH_2)(OH)^-$) by phosphate ($H_2PO_4^-$ and HPO_4^{2-}) and acetohydroxamic acid ($CH_3C(O)N(OH)H$) were investigated. The phosphate reactions were found to be pH dependent in the range of 4–8. Phosphate substitution rates are independent of the degree of phosphate protonation, and pH dependence is due to the difference in reactivity of $Fe(NTA)(OH_2)_2$ ($k = 3.6 \times 10^5$ M^{-1} s^{-1}) and $Fe(NTA)(OH_2)(OH)^-$ ($k = 2.4 \times 10^4$ M^{-1} s^{-1}). Substitution by acetohydroxamic acid is insensitive to pH in the range of 4–5.2, and $Fe(NTA)(OH_2)_2$ and $Fe(NTA)(OH_2)(OH)^-$ react at equivalent rates ($k = 4.2 \times 10^4$ and 3.8×10^4 M^{-1} s^{-1}, respectively). Evidence for acid-dependent and acid-independent back-reactions was obtained for both the phosphate and acetohydroxamate complexes. Reactivity patterns were analyzed in the context of NTA labilization of coordinated water, and outer-sphere electrostatic and H-bonding influences were analyzed in the precursor complex (K_{os}).

Introduction

Nitrilotriacetic acid (NTA) is one of the most widely used and studied organic chelating agents.[1] Major commercial use includes application as a detergent builder. NTA is a tetradentate ligand, and consequently, hexacoordinated metals such as iron can form ternary complexes with NTA and other mono- and bidentate ligands found in the environment. The presence of iron as the second most prevalent metal on the earth's surface and the high occurrence of NTA and phosphate in the environment due to industrial activity and agricultural runoff makes an investigation of the kinetics and mechanism of Fe−NTA interactions with phosphate of interest. The thermodynamics of metal−NTA−phosphate complex systems have been extensively studied.[2−4] Unfortunately, very few kinetic or mechanistic data are available for Fe−NTA ternary complex formation.[5] An additional impetus for our study is the wide use of Fe(III)NTA complexes for in vitro biophysical studies as Fe(III) donors or buffers to prevent hydrolysis and precipitation of iron hydroxides and oxides at physiological pH. Here we report on the kinetics and mechanism of Fe(NTA) ternary complex formation with phosphate and acetohydroxamic acid (ACH).

Experimental Section

Materials. Deionized water was used in all experiments. Stock solutions of NaOH (Fisher), NTA (Acros), PIPES (Acros), MES (Sigma-Aldrich), ACH (Sigma-Aldrich), and Na_2HPO_4 (Sigma-Aldrich) were used without further purification. A stock solution of $NaClO_4$ was prepared from anhydrous $NaClO_4$ (Sigma-Aldrich), filtered, and standardized by passage through a DOWEX 50W−X8 strong-acid cation-exchange column in H^+ form by titration against standard NaOH to the phenolphthalein end point. A Fe−NTA solution (Fe:NTA 1:1) was prepared by slow addition of the appropriate volume of acidic $Fe(ClO_4)_3$ stock solution (0.087 M Fe^{3+}/0.1 M $HClO_4$) to a vigorously stirred solution of NTA in an appropriate buffer (PIPES buffer for pH = 4, 7.5, and 8; MES buffer for all other pHs). The resulting $Fe(NTA)_{(aq)}^{m-}$ solutions were allowed to stabilize after preparation for at least 1 h. Fe−NTA species distributions were computed using the Hyperquad Simulation and Speciation Program (Protonic Software).

Physical Measurements. Spectral studies were performed using a Varian Cary 100-Bio UV−vis spectrophotometer, and kinetic studies were performed using an Applied Photophysics stopped-flow (SX.18 MV) equipped with a diode array spectrophotometer with an approximate range of 380−750 nm. The kinetics of phosphate and ACH ligand exchange reactions were studied by following the increase in the absorbance at 310 and 438 nm, respectively. The effect of phosphate and ACH on the exchange

* Address correspondence to this author. E-mail: alvin.crumbliss@duke.edu. Fax: 919-660-1605.

(1) Novack, B. *Environ. Sci. Technol.* **2002**, *36*, 4009.
(2) Arp, A. P.; Mayer, W. L. *Can. J. Chem.* **1985**, *63*, 3357.
(3) Lente, G.; Elizabeth, A.; Magalhães, A.; Fabian, I. *Inorg. Chem.* **2000**, *39*, 1950.
(4) Al-Sogair, F.; Marafie, H. M.; Shuaib, N. D.; Youngo, H. B.; El-Elzaby, M. S. *J. Coord. Chem.* **2002**, *55*, 1097.
(5) Das, K. B.; Bhattacharya, S. G.; Banerjee, D. *J. Coord. Chem.* **1989**, *19*, 311.

10.1021/ic026281o CCC: $25.00
Published on Web 05/28/2003

Scheme 1

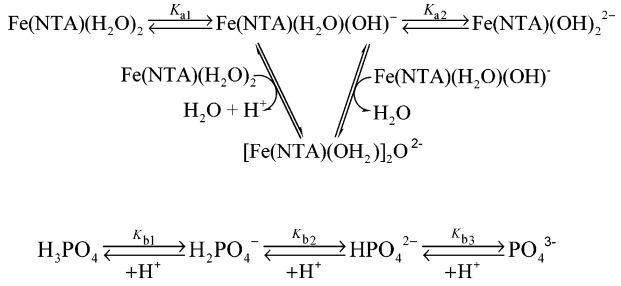

kinetics were examined by varying the ligand and H^+ concentrations. All measurements were performed under pseudo-first-order conditions of excess ligand, at 25 °C, and constant ionic strength, $I = 0.1$ ($NaClO_4$). Absorbance data were analyzed using Applied Photophysics kinetic software. pH measurements were performed using an Orion pH meter (model 230 A).

Results

General Observations. Scheme 1 shows the proton- and concentration-dependent equilibria rapidly established over the course of our reaction conditions (pH = 3.97−8.01 and $[Fe(III)]_{TOT} = 0.05-0.2$ mM).

Equilibrium data in the literature show that under our experimental conditions, only one phosphate molecule is bound per molecule of Fe(NTA).[6] The overall reaction under investigation is shown in eq 1, where $Fe(NTA)_{(aq)}^{m-}$ and $H_xPO_4^{n-}$ represent the various hydrolyzed and protonated forms of the reactants, depending on pH, as illustrated in Scheme 1. Reaction 1 was observed to proceed in two steps. The faster step ($t_{1/2} \approx 10$ ms) is characterized by an increase in absorbance, which was monitored at 310 nm (shoulder) and whose rate depends on the phosphate concentration. The slower step ($t_{1/2} \approx 5-10$ s) is characterized by a decrease in absorbance at 310 nm and no dependence on the rate of phosphate concentration. A 4-fold increase in concentration of $Fe(NTA)_{(aq)}^{m-}$ increases the dimer concentration as a minor component by a factor of 15[7] (from <0.15% to 2.5%; Scheme 1) and has no influence on the rate or amplitude of the first step. In a blank reaction without phosphate present (i.e., dilution of $Fe(NTA)_{(aq)}^{m-}$), only the second step appears. On the basis of these observations, the second step can be attributed to the monomer−dimer equilibrium of $Fe(NTA)_{(aq)}^{m-}$ [8] (Scheme 1) and has no influence on the first step, which is assigned to reaction (1).

$$Fe(NTA)_{(aq)}^{m-} + H_xPO_4^{n-} \rightarrow Fe(NTA)H_xPO_{4(aq)}^{p-} \quad (1)$$

Reaction 1 was also carried out with acetohydroxamic acid (ACH) in place of phosphate. Under pseudo-first-order conditions (ACH in excess), two steps were also observed. At pH = 3.95, the first step has a $t_{1/2} \approx 2$ ms and the second step has $t_{1/2} \approx 7$ s. Product spectra obtained after both steps have the same λ_{max} at 438 nm in the range of [ACH] used.

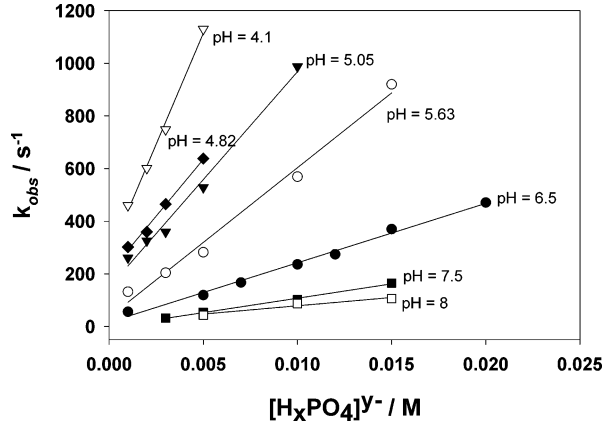

Figure 1. Plots of k_{obs} vs $[H_xPO_4]^{y-}$ concentration for reaction 1 at different pH. Conditions: [Buffer] = 50 mM, $[Fe(NTA)_{(aq)}] = 0.1$ mM, $I = 0.1$, $T = 25$ °C.

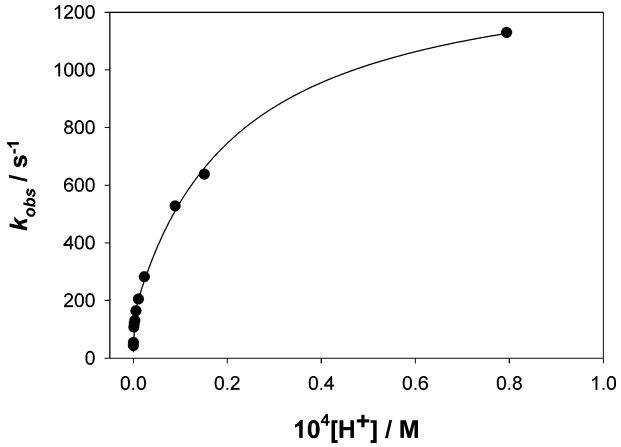

Figure 2. Plot of k_{obs} vs $[H^+]$ concentration for reaction 1. The solid line corresponds to a fit of eq 3 to the data. Conditions: $[H_xPO_4]^{y-} = 5$ mM, [Buffer] = 50 mM, $[Fe(NTA)_{(aq)}^{m-}] = 0.1$ mM, $I = 0.1$, $T = 25$ °C.

At pseudo-first-order conditions, when $Fe(NTA)_{(aq)}^{m-}$ is in excess, only the first step appears. Spectral maxima and the rate are the same as in the first step in the experiments when ACH is in excess and can be attributed to the same process. However, at pH = 5.63 and at a large excess of ACH ([ACH] = $100[Fe(NTA)_{(aq)}^{m-}]$), the λ_{max} of the product after the second step shifts to 426 nm ($\epsilon \approx 2560$ M^{-1} cm^{-1}). The λ_{max} and ϵ are consistent with formation of tris(acetohydroxamato)Fe(III).[9] According to these observations, we assigned the first step to the formation of a ternary complex, (Fe−NTA−ACH), and the subsequent step to the formation of a bis(acetohydroxamato)Fe(NTA) ternary complex and/or tris-(hydroxamato)Fe(III).

All data and mechanistic interpretations presented are related to the first step of reaction 1 for both the phosphate and ACH substitution reactions.

Phosphate Substitution at $Fe(NTA)_{(aq)}^{m-}$. The kinetics of reaction 1 were investigated under pseudo-first-order conditions at excess total phosphate concentration. Figure 1 shows a linear dependence of k_{obs} on the phosphate concentration at all pH values investigated. At low pH, the intercepts are non-zero and approach zero with increasing pH. The

(6) Yanez-Sedano, P.; Cabrera-Martin, A.; Gallego-Andreu, R. *An. Quim., Ser. B* **1986**, *82*, 90.
(7) Sanchiz, J.; Esparza, P.; Dominguez, S.; Brito, F.; Mederos, A. *Inorg. Chim. Acta* **1999**, *291*, 158.
(8) Gilmour, A. D.; Cassidy, J. K.; McAuley, A. *J. Chem. Soc. A* **1970**, 2847.
(9) Biruš, M.; Bradić, Z.; Kujundžić, N.; Pribanić, M.; Wilkins, P. C.; Wilkins, R. G. *Inorg. Chem.* **1985**, *24*, 3980.

Scheme 2

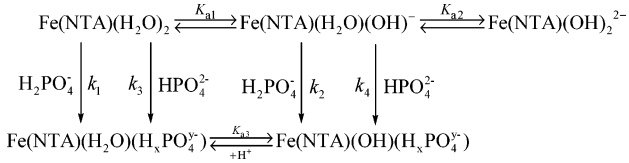

Scheme 3

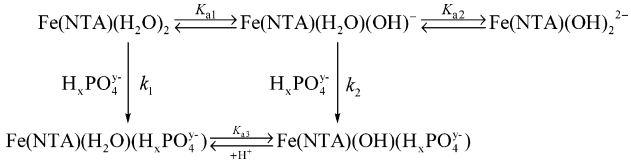

proton dependence of k_{obs} shows saturation behavior with increasing [H^+] (Figure 2).

Both phosphate and $Fe(NTA)_{(aq)}^{m-}$ exist in variable degrees of protonation over the range of experimental conditions covered in our study (Scheme 1). The major forms of $Fe(NTA)_{(aq)}^{m-}$ are $Fe(NTA)(H_2O)_2$, $Fe(NTA)(H_2O)(OH)^-$, and $Fe(NTA)(OH)_2^{2-}$.[10] If we assume that the reactive species are $H_2PO_4^-$, HPO_4^{2-}, $Fe(NTA)(H_2O)_2$, and $Fe(NTA)(H_2O)(OH)^-$, as illustrated in Scheme 2,[11] then k_{obs} for reaction 1 in the presence of excess phosphate may be described as depicted in eq 2, where K_{a1}, K_{a2}, K_{b1}, and K_{b2} are equilibrium constants defined in Scheme 1 and [$H_xPO_4^{n-}$] represents the total phosphate concentration.

$$k_{obs} = \frac{\left[H_xPO_4^{y-}\right]}{1+\frac{K_{b2}}{[H^+]}+\frac{[H^+]}{K_{b1}}}\left(\frac{k_1}{1+\frac{K_{a1}}{[H^+]}+\frac{K_{a1}K_{a2}}{[H^+]^2}}+\frac{k_2}{1+\frac{K_{a2}}{[H^+]}+\frac{[H^+]}{K_{a1}}}\right) + \frac{\left[H_xPO_4^{y-}\right]}{1+\frac{[H^+]}{K_{b1}}+\frac{[H^+]^2}{K_{b1}K_{b2}}}\left(\frac{k_3}{1+\frac{K_{a1}}{[H^+]}+\frac{K_{a1}K_{a2}}{[H^+]^2}}+\frac{k_4}{1+\frac{K_{a2}}{[H^+]}+\frac{[H^+]}{K_{a1}}}\right)+k_{-1}[H^+] \quad (2)$$

Fitting eq 2 to all of the kinetic data gives very similar values for k_1 and k_3 and for k_2 and k_4 ($k_1 \approx k_3 = 2.3 \times 10^5$ M^{-1} s^{-1}; $k_2 \approx k_4 = 1.4 \times 10^4$ M^{-1} s^{-1}), suggesting identical reactivity for the phosphate species independent of the degree of protonation. Additionally, in the pH range from 5.3 to 3.9, k_{obs} increases considerably (Figure 2) whereas the phosphate speciation is almost unchanged in the same pH range (over 98% of all phosphate present is $H_2PO_4^-$). Therefore, the increase in k_{obs} is assigned to a difference in reactivity of the different $Fe(NTA)_{(aq)}^{m-}$ species and is not due to different reactivity of the phosphate species. The mechanism can be simplified and is depicted in Scheme 3.

The rate law for Scheme 3 is shown in eq 3, where $H_xPO_4^{y-}$ is the total concentration of all the protonated forms of phosphate and k_1 and k_2 are the microscopic rate constants for ligation of $Fe(NTA)(H_2O)_2$ and $Fe(NTA)(H_2O)(OH)^-$, respectively. K_{a1} and K_{a2} are equilibrium constants defined in Scheme 3. From the pH dependence of the intercepts (Figure 1), it is evident that the back-reaction is proton driven. Fitting eq 3 to all of the data yields the microscopic rate constants: $k_1 = 3.6(4) \times 10^5$ M^{-1} s^{-1} and $k_2 = 2.4(4) \times 10^4$ M^{-1} s^{-1}. The goodness of fit is illustrated in Figure S1 of the Supporting Information. In the fitting procedure, K_{a1} and K_{a2} were also treated as variables, and the values obtained ($pK_{a1} = 4.36$ and $pK_{a2} = 7.58$) are in excellent agreement with literature data for similar experimental conditions ($pK_{a1} = 4.36$ and $pK_{a2} = 7.39$).[10] This provides additional support for the validity of Scheme 3. The addition of the term for the back-reaction in the scheme did not improve the fit, and the resulting microscopic rate constants exhibit a large standard deviation. With our experimental conditions an accurate value for the reverse rate constant cannot be obtained, other than the observation that it is proton driven. The rate constants for Scheme 3 are compiled in Table 1.

$$k_{obs} = \left[H_xPO_4^{y-}\right]\left(\frac{k_1}{1+\frac{K_{a1}}{[H^+]}+\frac{K_{a1}K_{a2}}{[H^+]^2}}+\frac{k_2}{1+\frac{K_{a2}}{[H^+]}+\frac{[H^+]}{K_{a1}}}\right)+k_{-1}[H^+] \quad (3)$$

Acetohydroxamic Acid Substitution at $Fe(NTA)_{(aq)}^{m-}$. The ligation reaction for $Fe(NTA)_{(aq)}$ with ACH was investigated at pH = 3.95 and 5.24. The pK_a of ACH is 9.02[12], and consequently over this pH range, this ligand exists only in the protonated form. A linear dependence of k_{obs} with [ACH] is observed (Figure 3), and the parallel slopes at different pH values indicate essentially identical reactivity. The intercepts can be attributed to parallel proton independence and dependence on the reverse reactions. Ternary complex formation and dissociation is illustrated in Scheme 4 (HL represents ACH).

The rate law for Scheme 4 in the presence of excess [HL] is shown in eq 4. Equation 4 was fit to the data (Supporting Information, Figure 2S) when K_{a1} and K_{a2} (defined in Scheme 1) were fixed according to literature values,[10] and the results are summarized in Table 1. When K_{a1} and K_{a2} were treated as variable parameters, the values obtained were consistent with published values,[10] which supports our mechanistic interpretation in Scheme 4.

$$k_{obs} = [HL]\left(\frac{k_5}{1+\frac{K_{a1}}{[H^+]}+\frac{K_{a1}K_{a2}}{[H^+]^2}}+\frac{k_6}{1+\frac{K_{a2}}{[H^+]}+\frac{[H^+]}{K_{a1}}}\right)+k_{-5}[H^+]+k_{-6} \quad (4)$$

Discussion

Data in the literature readily demonstrate that substitution of water ligands in the first-coordination shell of Fe(III) by strong electron pair donors enhances the ligand exchange reactivity of the remaining aquo ligands. This may be illustrated by comparing rate constants for water exchange at $Fe(H_2O)_6^{3+}$ (1.7×10^2 s^{-1})[13] and $Fe(H_2O)_5OH^{2+}$ ($1.4 \times$

(10) Motekaitis, R. J.; Martell, A. E. *J. Coord. Chem.* **1994**, *31*, 67.
(11) When $Fe(NTA)(OH)_2^{2-}$ was included as a reactive species for direct reaction with $H_xPO_4^{y-}$, parameter convergence did not occur, and consequently, its participation beyond the H^+-dependent equilibrium shown in Scheme 2 was not considered. PO_4^{3-} was omitted from consideration as a reactive species because of its negligible concentrations over the pH range investigated.
(12) Monzyk, B.; Crumbliss, A. L. *J. Org. Chem.* **1980**, *45*, 4670.
(13) Swaddle, T. W.; Merbach, A. E. *Inorg. Chem.* **1981**, *20*, 4212.

Table 1. Rate Constants for Complexation of $Fe(NTA)(H_2O)_2$ and $Fe(NTA)(H_2O)(OH)^-$ with Phosphate and Acetohydroxamic Acid[a]

	phosphate	acetohydroxamic acid	
	$10^{-4}\,k/M^{-1}\,s^{-1}$	$10^{-4}\,k/M^{-1}\,s^{-1}$	k
$Fe(NTA)(H_2O)_2$	36(4) (k_1)[b]	4.2(6) (k_5)[c]	$4.5(2)\times10^6\,M^{-1}\,s^{-1}$ (k_{-5})[c]
$Fe(NTA)(H_2O)(OH)^-$	2.4(4) (k_2)[b]	3.8(3) (k_6)[c]	$1.8(2)\times10^2\,s^{-1}$ (k_{-6})[c]

[a] Conditions: $T = 25$ °C; $I = 0.1$ ($NaClO_4$). Numbers in parentheses are standard deviations of the last digit. [b] Microscopic rate constants defined in Scheme 3 and determined from nonlinear least-squares analysis of kinetic data according to eq 3. [c] Microscopic rate constants defined in Scheme 4 and determined from nonlinear least-squares analysis of kinetic data according to eq 4.

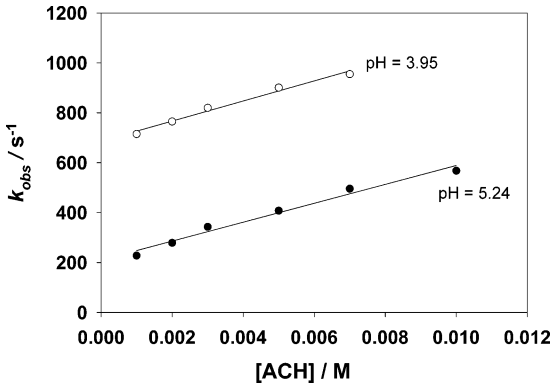

Figure 3. Plots of k_{obs} vs acetohydroxamic acid concentration at different pH. Conditions: [Buffer] = 50 mM, $[Fe(NTA)_{(aq)}{}^{m-}] = 0.1$ mM, $I = 0.1$, $T = 25$ °C.

Scheme 4

$$Fe(NTA)(H_2O)_2 + HL \underset{k_{-5}}{\overset{k_5}{\rightleftharpoons}} Fe(NTA)L + H^+$$

$$Fe(NTA)(H_2O)(OH)^- + HL \underset{k_{-6}}{\overset{k_6}{\rightleftharpoons}} Fe(NTA)L + H_2O$$

$10^5\ s^{-1}$),[13] and the second-order rate constants for reaction of $Fe(H_2O)_6{}^{3+}$ with a first ($1.2\ M^{-1}\,s^{-1}$) and second ($2\times10^3\ M^{-1}\,s^{-1}$) equivalent of *N*-methylacetohydroxamic acid.[14] These reactions are expected to be dissociatively activated (I_d) so that their rates are largely controlled by the lability of the coordinated H_2O.

These considerations are consistent with the observed rate constants for the reaction of phosphate and ACH with $Fe(NTA)(H_2O)_2$ (Table 1), which are several orders of magnitude greater than the corresponding reaction with $Fe(H_2O)_6{}^{3+}$ or $Fe(H_2O)_5OH^{2+}$.[3,9,14] The second-order rate constants reported here for aquo-ligand substitution at $Fe(NTA)(H_2O)_2$ ($10^4-10^5\ M^{-1}\,s^{-1}$; Table 1) suggest a strong labilizing influence for the tetradentate NTA^{3-} ligand in the first coordination shell of Fe(III). For example, the corresponding second-order rate constant for the reaction of $Fe(TIRON)_2(H_2O)_2{}^{5-}$ with TIRON to form $Fe(TIRON)_3{}^{9-}$ is $7.7\times10^3\ M^{-1}\,s^{-1}$,[15] and for the reaction of $Fe(CH_3C(O)N(O)H)_2(OH_2)_2{}^{+}$ with ACH to form $Fe(CH_3C(O)N(O)H)_3$, the corresponding second-order rate constant is $1.7\times10^3\ M^{-1}\,s^{-1}$.[9] It is unclear why the rate constant (k_1; Table 1) for the reaction of phosphate anion with $Fe(NTA)(H_2O)_2$ is an order of magnitude faster than the rate constant (k_5; Table 1) for the corresponding ACH reaction, given that these are expected to be dissociatively activated reactions.[16] Hydrogen bonding of the phosphate anion with an aquo ligand in the precursor complex may serve to enhance the substitution rate.

Incorporation of OH^- in the first coordination shell of $Fe(NTA)(H_2O)_2$ to form $Fe(NTA)(H_2O)(OH)^-$ does not enhance aquo-ligand substitution rates (Table 1). This is consistent with previous observations that the labilizing effect of anionic chelates in the first-coordination shell of Fe(III) is saturated after two coordination sites are occupied by strong electron pair donors. For example, the second-order rate constants for steps 2 and 3 (eq 5)

$$Fe(H_2O)_6{}^{3+} + L \xrightarrow{Step\ 1} FeL(H_2O)_4 + L \xrightarrow{Step\ 2} FeL_2(H_2O)_2 + L \xrightarrow{Step\ 3} FeL_3 \quad (5)$$

(charges omitted for clarity) are comparable in tris complex formation from $Fe(H_2O)_6{}^{3+}$ by ACH,[9] *N*-methylacetohydroxamic acid,[14] and TIRON.[15] This suggests saturation of the aquo-ligand labilizing effect after the formation of $FeL(H_2O)_4{}^{n+}$. Why $Fe(NTA)(H_2O)(OH)^-$ reacts with a phosphate anion with a second-order rate constant an order of magnitude less than the reaction with $Fe(NTA)(H_2O)_2$ is open to speculation. As noted above, this may be due to enhanced reactivity with $Fe(NTA)(H_2O)_2$ because of H-bonding in the precursor complex. This may also be due to an electrostatic influence on the precursor complex formation constant, K_{OS}. Using the Fuoss equation,[17] we estimate that K_{OS} is diminished by a factor of 3 ($0.3\ M^{-1}-0.1\ M^{-1}$) for a phosphate anion reacting with anionic $Fe(NTA)(H_2O)(OH)^-$ rather than neutral $Fe(NTA)(H_2O)_2$. Calculated K_{OS} values for anionic $Fe(NTA)(H_2O)(OH)^-$ reactions with $H_2PO_4^-$ and HPO_4^{2-} vary somewhat (0.18 and $0.1\ M^{-1}$, respectively). A statistical factor may also be operative because the number of labile aquo ligands diminishes by a factor of 2 when comparing $Fe(NTA)(H_2O)_2$ with $Fe(NTA)(H_2O)(OH)^-$.

In summary, we find that first-coordination shell labilization effects of NTA and second-coordination shell electrostatics and H-bonding differentially influence the dissociatively activated rapid ternary complex formation of $Fe(NTA)(OH_2)_2$ and $Fe(NTA)(OH_2)(OH)^-$ with phosphate and ACH.

Acknowledgment. We thank the NSF for financial support (CHE-0079066) and the Fulbright Association for a fellowship to M.G.

Supporting Information Available: Plot of $k_{calculated}$ vs $k_{observed}$ for reaction (1) analyzed using eq 3. This material is available free of charge via the Internet at http://pubs.acs.org.

IC026281O

(14) Caudle, M. T.; Crumbliss, A. L. *Inorg. Chem.* **1994**, *33*, 4077.
(15) Zhan, Z.; Jordan, R. B. *Inorg. Chem.* **1996**, *35*, 1571.
(16) Biruš, M.; Bradić, Z.; Kujundžić, N.; Pribanić, M. *Prog. React. Kinet.* **1993**, *18*, 173.
(17) Fuoss, R. M. *J. Am. Chem. Soc.* **1958**, *80*, 5059.